Flexible Chains of Ferromagnetic Nanoparticles

James Townsend, Ruslan Burtovyy,* Yuriy Galabura, and Igor Luzinov*

Department of Materials Science and Engineering, Clemson University, 161 Sirrine Hall, Clemson, South Carolina 29634, United States

ABSTRACT We report the fabrication of flexible chains of ferromagnetic Ni nanoparticles that possess the ability to adapt other than the typically observed rigid (nearly) straight configurations in the absence of an external magnetic field. The dynamic mobility of the ferromagnetic chains originates from a layer of densely grafted polyethylene glycol macromolecules enveloping each nanoparticle in the chain. While ferromagnetic chains of unmodified Ni nanoparticles behave as stiff nickel nanorods, the chains made of the grafted nanoparticles demonstrate extreme flexibility. Upon changing the direction of the field, and inevitably going through a zero-field point, the shorter chains undergo chain—globule—chain transformation. The longer chains can bend to a high degree, attaining "snake-like" configurations.

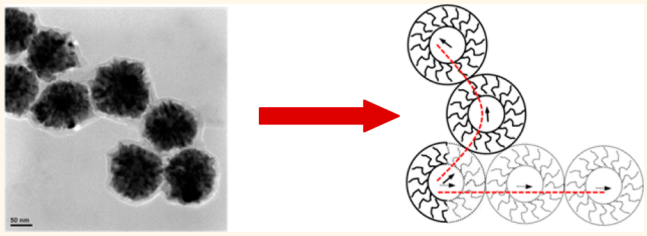

KEYWORDS: ferromagnetic chains · nickel nanoparticles · ferromagnetic nanoparticles · magnetic field · surface modification · grafting to · polymer brush

The collective behavior of colloidal particles in a liquid medium is one of the major parameters that determine the structure and properties (rheology, texture, and/or functionality) of nanoparticle-based composites, multiphase systems, and devices.[1−4] To this end, the assembly of colloidal nanoparticles into extended micrometer-size chains through the utilization of chemical reactions, interfacial interactions, and/or electric/magnetic fields to overcome thermal fluctuations has been extensively explored.[2−12] In particular, there is a significant interest in the magnetic assembly of ferromagnetic particles, which provides selective directionality *via* dipolar associations.[13] Nanoparticles (Ni, Co) have been intensively studied for their potential biomedical,[14−19] electronic,[20] sensoric,[21−25] and magneto-rheological/ferrofluidic[26−28] applications. It is demonstrated, both theoretically and experimentally, that magnetic fields generate strong dipole—dipole interactions, causing the particles to assemble in 2D and 3D arrays/chains.[3,4,7,26,29−33]

Important characteristic of the chains made of magnetic particles is their ability to change conformation when an external magnetic field is turned on/turned off or changes direction. To this end, the flexibility of the magnetic chains was studied both theoretically and experimentally.[34−44] For instance, Cebers reviewed advancements in the field of flexible magnetic filaments and proposed that unifying approach for the description of their behavior in various static and dynamic conditions is possible on the basis of an extended Kirchhoff model of an elastic rod.[35] Dreyfus *et al.*[34,37] and Gauger and Stark[36] demonstrated that (when a time-varying magnetic field is applied) micrometer-sized paramagnetic particles connected by polymer bridges are capable of propelling themselves through a fluid *via* bending motions. Goubault *et al.*[45] reported that long flexible filaments, made of superparamagnetic submicron particles linked by polymer chains, can adopt under magnetic field a hairpin configuration. The hairpins' curvature can be reversibly controlled by the intensity of magnetic field. Biswal and Gast[38−40] studied in detail actuation of chains made of paramagnetic colloidal particles connected with flexible polyethylene glycol macromolecules. It was shown that the chains can be magnetically actuated to manipulate microscopic fluid flow. The flexibility of the chains can be adjusted by varying the length of the linker molecule.

The key characteristics of the ferromagnetic nanoparticle arrays, distinguishing them from their paramagnetic counterparts, are the

* Address correspondence to rburtov@clemson.edu, luzinov@clemson.edu.

Received for review April 1, 2014 and accepted June 20, 2014.

Published online June 20, 2014
10.1021/nn501787v

quasi-irreversibility of the chain formation process and their significant rigidity.[13] The integrity of the chains without chemical linkers and their rigidity is a direct consequence of strong magnetic interaction between the particles. There have been limited experimental results reported in the scientific literature demonstrating any considerable dynamic changes of the chain conformation composed of ferromagnetic nanoparticles. In this respect, Pyun *et al.* studied fabrication and behavior of ferromagnetic chains containing polystyrene-coated Co nanoparticles (PS-CoNPs).[41−44] It was demonstrated that the nanoparticles self-assemble into chains at an oil/water interface under zero-field conditions.[42] The conformation of the chains strongly resembled the self-avoiding random walk of organic macromolecules. When placed atop a permanent magnet, the PS-CoNPs form dense arrays of 1-D chains that look like biological cilia.[41,44] The arrays could be actuated with an external magnetic field. The PS-CoNPs chain can be also attached to a larger Fe_3O_4 nanoparticle to form flagella-like nanoparticle assembly.[43] The cyclical bending of the PS-CoNPs chain, propelling the assembly, was observed when a sinusoidal magnetic field was applied.

Herein, we describe the fabrication of flexible chains of ferromagnetic Ni nanoparticles that possess the ability to adapt in different ways other than the typical rigid (nearly) straight configurations in the absence of an external magnetic field. The chains obtained orient in a magnetic field, forming magnetic rods. However, they collapse into globules upon removal of the magnetic field. The reapplication of the magnetic field causes the collapsed chain to unfold, restoring rod orientation along the field. To the best of our knowledge, it is the first time that such extreme flexibility has been demonstrated for chains of Ni ferromagnetic particles.

In essence, the flexibility of the ferromagnetic particle chains in the system originates from a layer of grafted polyethylene glycol (PEG) macromolecules enveloping each nanoparticle in the chain. The densely grafted macromolecules form a polymer brush on the Ni particles, where the constrained geometrical environment limits the available space the polymers can occupy, forcing the chains to stretch normally to the surface.[46,47] The polymer brush provides a steric repulsive barrier around the nanoparticles, preventing their aggregation, regulating the distance between nanoparticles in the ferromagnetic chains, and allowing for the rotation of particles in the chains. Therefore, the polymer layer enables the arrays and chains to be flexible, creating magnetic morphologically varying nanostructures.

We foresee that the flexible ferromagnetic chains will allow creating responsive magnetic materials in which the switching behavior and the permanent magnetic moment coexist. The potential applications for these particles can close the gap between ferrofluids, with small superparamagnetic nanoparticles, and magneto-rheological fluids, with large ferromagnetic particles. This allows for a much broader base of application: nanovalves, microstirrers, hyperthermia treatments, drug delivery, magnetic sensors, braking fluids, energy storage, energy generation, and γ-radiation protection. These applications will revolve around flexible nanoparticle chains, with properties tailored using the specific grafted polymer layers.

RESULTS AND DISCUSSION

Nickel Ferromagnetic Nanoparticles. The particles synthesized were nearly spherical and 100 ± 10 nm in size (Figure 1a,b). The surface of the particles was quite rough, as typically found for Ni nanoparticles obtained *via* the reduction procedures employed.[48] The XRD pattern (Figure 1c) clearly indicated the presence of a single face-centered cubic crystal phase with only three characteristic peaks (2θ = 44.6, 52.0, and 76.5°) corresponding to pure metallic nickel.[49] No nickel oxide was detected within the XRD detection limit. Considering that the detection limit for XRD is a few percent for mixtures,[50] ∼1−2 nm of oxide layer for 100 nm particles might be present on the surface of the nanoparticles. A film of such thickness can be attributed to a natural oxide layer that inevitably forms on the surface of nanoparticles. The absence of the nickel oxide line in the XRD pattern suggested that no additional nickel oxide (aside from that naturally formed on the surface) was present in the synthesized particles.

Magnetic measurements (Figure 1d) confirmed the ferromagnetic nature of the material, with saturation magnetization of about 30 emu/g and remnant magnetization and coercivity of 7.1 emu/g and 90 Oe, respectively. The values differ from those for bulk Ni[51] but are similar to the results reported for Ni nanoparticles in the scientific litearture.[48,52]

Grafted Layer. The design of the grafted layer to generate flexible chains of ferromagnetic nanoparticles requires an understanding of the chain formation process and the particle−particle interaction within the chain. The chain made of bare Ni nanoparticles can be considered as a single dipole or magnetic nanorod, where particles are in direct contact because of strong magnetic forces (Figure 2a). The magnetic interaction energy in the chain is much larger than the thermal energy. Therefore, even after reduction/elimination of the external magnetic field, the chain does not disintegrate or changes its conformation. The introduction of flexibility into the chain involves a significant decrease in the magnetic dipole−dipole interaction as well as incorporation of components possessing an intrinsic flexibility/lubricating ability on the surface of the particles. Both these requirements can be satisfied by surface modification of the particles with a polymer brush.[53−55] The surfaces/nanoparticles covered with

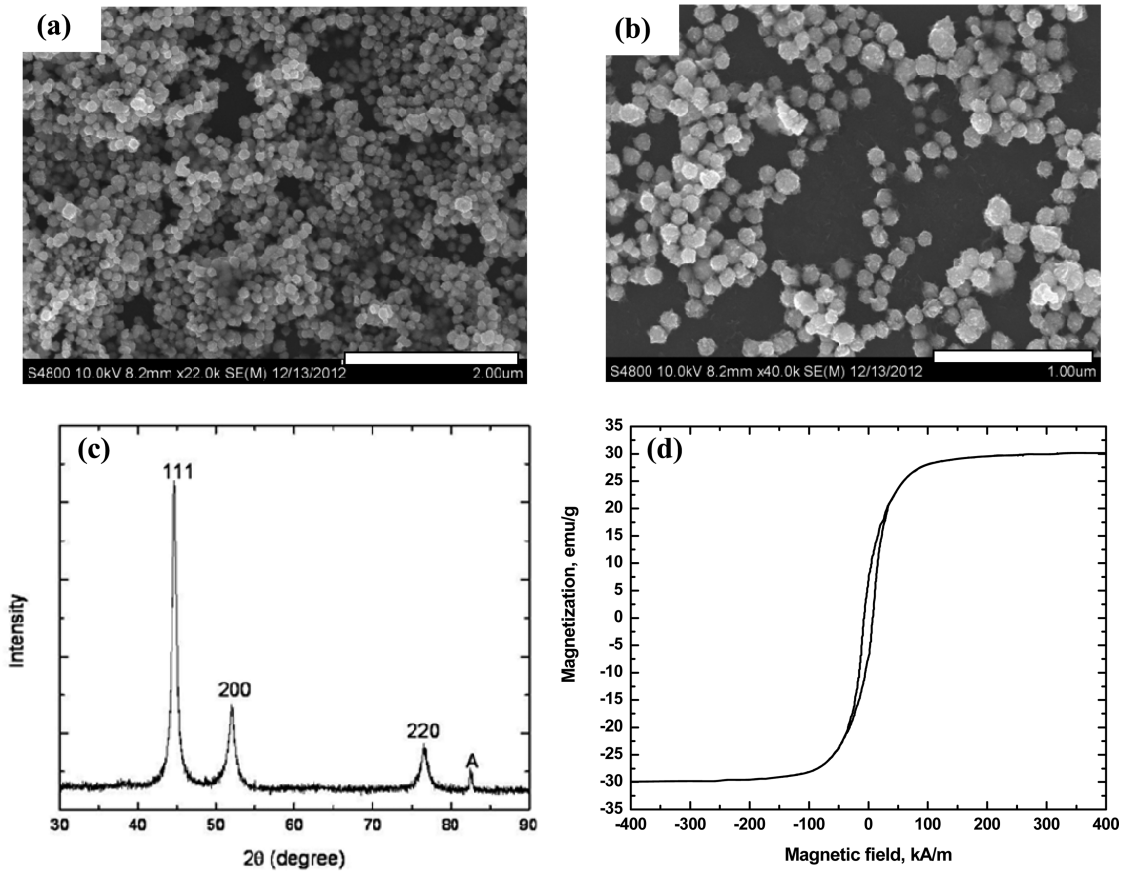

Figure 1. (a,b) SEM images of the synthesized Ni nanoparticles: scale bar = (a) 2 μm and (b) 1 μm. (c) XRD pattern of the synthesized Ni nanoparticles. (d) Magnetization *vs* strength of magnetic field for the Ni nanoparticles.

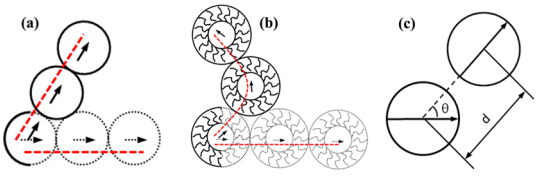

Figure 2. Schematic representation of a predicted change in the shape of chains formed by (a) unmodified and (b) modified particles after removal of magnetic field. (c). Schematic representation of 2D two-particle system used for calculation of magnetic interaction by eq 1.

the brushes are also known to sterically repel each other in a good solvent for the macromolecules constituting the grafted layers.[46,56−59]

Let us consider the influence of a polymer brush on the forces involved in the interaction between the ferromagnetic nanoparticles. First of all, the polymer-grafted layer prevents direct physical contact between the particles. Second, the attractive force that originated from the magnetic interaction is compensated by the repulsive steric force between the brush layers to a certain extent. In fact, the magnetic interaction energy scales as d^{-3} (where d is the distance between interacting dipoles). Therefore, a significant reduction in the magnetic component of interaction energy occurs upon an increase in distance between the particles.[60] When magnetic moments of individual particles are aligned (in the presence of an external magnetic field), the magnetic interactions are much stronger than thermal energy and preserving straight-chain configuration. However, in the absence of an external magnetic field, the decrease in the particle−particle attraction might allow particles to change position/slide relative to each other under the influence of thermal energy/motion (Figure 2b).

In this work, we selected polyethylene glycol for the grafting because the polymer is soluble in a significant number of organic solvents and in water with different pH values.[47,61] Therefore, the flexible ferromagnetic chains can function in different environments. In our previous research, we studied in detail the grafting of carboxy-terminated PEG macromolecules of different molecular weights to silicon surfaces and silica particles using a poly(glycidyl methacrylate) [PGMA] anchoring layer.[47,62−65] It was determined that employment of PEG possessing molecular weight of 5000 g/mol allows dense and thick PEG brushes to be obtained by the "grafting to" approach. Therefore, in this work, we synthesized brushes on the Ni nanoparticles using PEG chains with molecular weight of 5000 g/mol.

The conditions for the surface modification of the Ni nanoparticles with the PEG brushes were developed

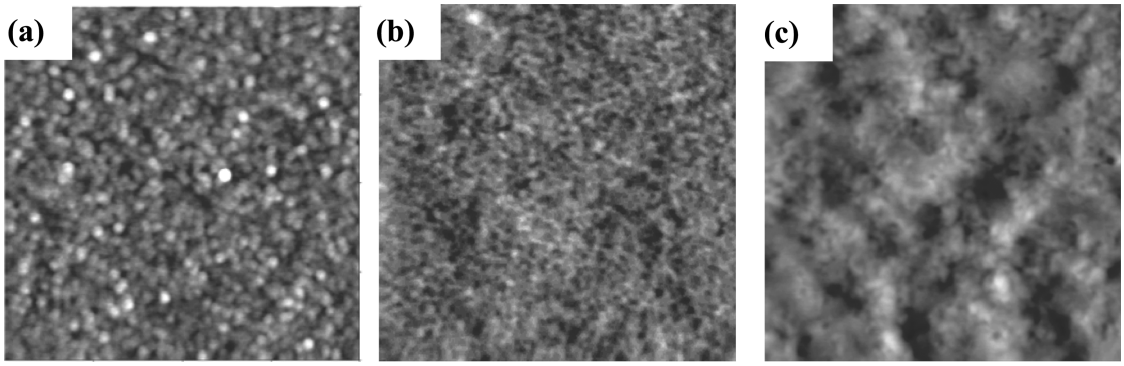

Figure 3. AFM topographical 1 × 1 μm images: (a) Ni film, (b) PGMA anchoring layer deposited on the Ni film, and (c) PEG brush grafted to the Ni film. Vertical scale 5 nm (a,b) and 20 nm (c).

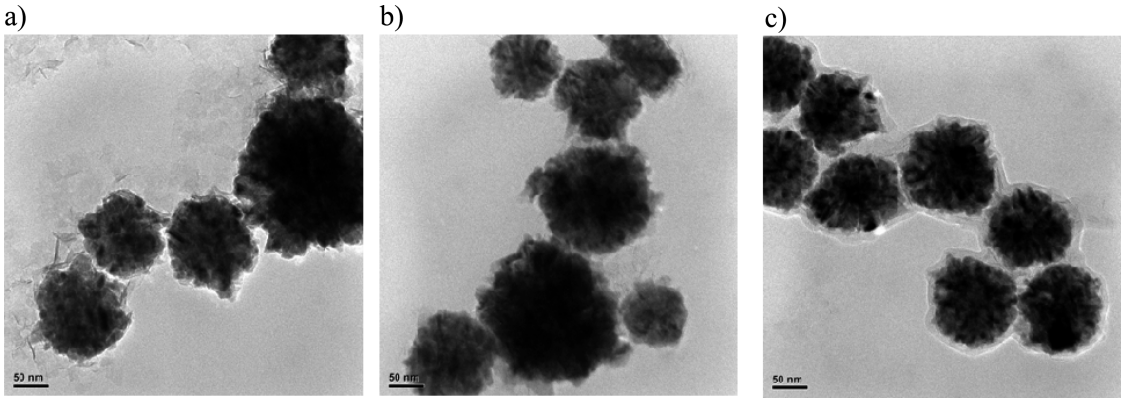

Figure 4. TEM images of (a) as-synthesized, (b) PGMA-modified, and (c) PEG-modified Ni nanoparticles (scale bar, 50 nm).

using model experiments with a flat substrate, a silicon wafer covered with Ni film. Every step of the modification of the wafer was monitored by ellipsometric measurements of the layer thickness and AFM imaging (Figure 3) of the grafted film. The PGMA anchoring layer on the surface of the Ni film was prepared by dip-coating the substrate from the PGMA solution. Annealing of the dip-coated film led to the formation of a 6−7 nm PGMA film on the substrate. We suggest that the PGMA monomeric units are anchored to Ni film *via* the coordination of the metal (from the nickel oxide located on the film surface) and opening of epoxy ring as described elsewhere.[66] The AFM studies revealed a smooth annealed PGMA layer that uniformly covered the substrate (Figure 3b). In the next step, carboxy-terminated PEG was grafted from melt to the substrate. Upon heating, the esterification reaction between PEG carboxy and PGMA epoxy groups resulted in the formation of the grafted PEG layer with a thickness of 12−13 nm. The AFM images demonstrated that the PEG layer was uniformly anchored to the surface (Figure 3c).

The grafting procedure developed for the flat Ni substrate was effectively used for the surface modification of the Ni nanoparticles. TEM images presented in Figure 4 confirm the successful modification of the particles. It is evident that, after modification with PEG, the particles were enveloped with about a 10−12 nm polymer shell (Figure 4c). The anchoring PGMA layer was not clearly visible (Figure 4b). We suggest that the smaller thickness of the layer as well as rough surface of the particles themselves obscured the visibility of the anchoring layer. After the PEG brush deposition, it was evident (from qualitative observation of coagulation kinetics) that the dispersibility of Ni nanoparticles in water was improved significantly. The particles were also found to be easy dispersible in a polar organic solvent (ethanol) and an aromatic organic solvent (toluene), indicating the universal compatibility character of the Ni nanoparticles (and chains made of them) modified with the grafted PEG layer.

We conducted theoretical estimations of the interaction energy between unmodified Ni particles and Ni particles modified with a polymer-grafted layer for a simplified 2D case. In our model (Figure 2c), the particle on the right rotates around the particle on the left. The magnetic interaction energy dependence on angle θ was calculated using eq 1, which is a form of the equation for magnetic dipoles interaction[60] simplified for the situation presented in Figure 2c:

$$E = -\frac{\mu_0}{2\pi d^3}\mu^2\cos\theta \qquad (1)$$

where μ_0 and μ are the magnetic constant and a particle's magnetic moment, respectively; d is the

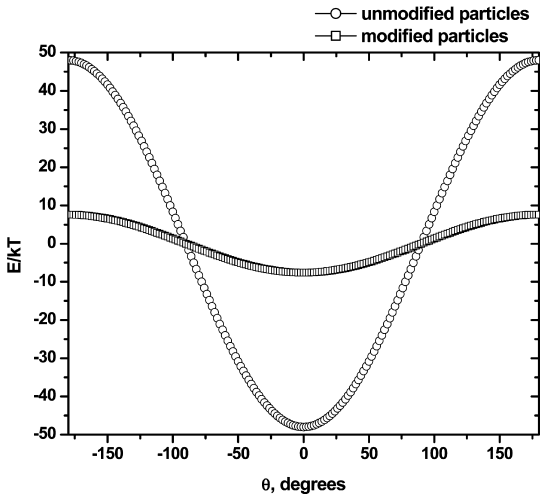

Figure 5. Dependence of magnetic component of interaction energy on the relative position of particles' magnetic dipoles.

distance between centers of the particles, and θ is the angle between particles' magnetic moments vectors. For our system, the distance between the centers of the unmodified Ni particles (d) was 100 nm for the direct contact case.

In the case of the modified particles, the PEG layer is swollen in water. Our previous investigations showed that in aqueous environment the PEG brush of 10−12 nm can extend up to ~40 nm.[63] Thus, the upper bound distance between the centers of the contacting Ni particles modified with the grafted layer can be estimated to be about 180 nm in our case. Therefore, the initial moment of interaction with maximum separation distance (180 nm) is provided to elucidate the influence of the PEG layer on the particle behavior in a ferromagnetic chain. In a real situation, the PEG layer might be somewhat compressed by the action of magnetic forces. The magnetic moment of the particles was set to be equal to remnant magnetization. It is the largest moment in the absence of the field. Therefore, our estimations represent the case of the strongest interaction between particles in the absence of the field. The starting point of the calculation is the complete alignment of the particles' moments.

Based on the theoretical analysis (Figure 5), there are several possible reasons for the different behavior of the modified with the grafting and bare original particles in the ferromagnetic chains. As-synthesized particles are characterized by a strong magnetic interaction (−50 kT) with rather steep potential walls for changing the relative position of magnetic moments. On the contrary, their modified counterparts are located initially in a shallow potential well on the order of kinetic energy (−8 kT). The depth of the well is significant in preventing a complete separation of the particles, but its shallow nature allows for significant changes in the relative position of the particles.

There are additional factors that contribute to the different behaviors of modified and unmodified particles, including van der Waals attractive forces. The forces add negative value to the already significant energy, restricting the particle rotation in the case of the bare particles coming in direct contact. At the same time, the forces are not present for the larger separation distance between the surfaces of the modified particles.[53] The steric repulsion forces between the particles covered with the grafted polymer chains positioned in a thermodynamically good solvent prevail over the attractive van der Waals forces between the grafted polymer chains in contact.[56]

If the limited particle rotation is still permissible for bare Ni particles from the energetic point of view, the presence of friction between the particles' surfaces can arrest otherwise energetically allowed movement. In fact, the roughness of the bare Ni nanoparticles' surface (Figure 4a) creates a potential barrier for movement through interlocking and anchoring of the opposite surfaces' features. Yet again, the situation is extremely favorable for the PEG-modified particles. The grafted layer smoothes the particle surface (Figure 2c). In addition, the friction forces between the grafted PEG layers in a good solvent are known to be very small[67,68] and would not prevent the particles from sliding/rolling.

The above discussion indicates the clear differences (summarized in Table 1) between two types of particles considered here and their behavior in a magnetic field. Analysis of the significant factors influencing this behavior suggested that the chains formed by PEG-modified Ni nanoparticles could possess flexibility.

Ferromagnetic Chains. The behavior of the chains formed by the original, nonmodified Ni nanoparticles, as well as by the particles modified with PEG brush, was followed in the presence and absence of a magnetic field. It was found that all Ni nanoparticles studied in this work start forming aggregates even in the absence of an external magnetic field. This behavior was theoretically predicted by de Gennes and Pincus, who demonstrated that, in the case of ferromagnetic particles having strong dipolar magnetic strength, the particles have a tendency to form clusters/chains depending on the density of the system.[4] The formation of the chains was also experimentally observed.[12,69] In fact, the presence of the magnetic field causes the ordering of the particle magnetic moments and the formation of the chains. As soon as a particle is located in the vicinity of other particles and theirs moments can interact, they engage in the chain formation process. Therefore, in contrast to paramagnetic particles, very small field strength is needed to start the chain formation process. An increase in the field strength (through the application of an external magnetic field) facilitates the kinetics of chain formation.

TABLE 1. Differences between the Unmodified and PEG-Brush-Modified Ferromagnetic Ni Particles Influencing Flexibility of the Chains Formed

factor	unmodified particles	PEG-modified particles
direct contact between the particle surfaces	present	replaced with contact between the swollen PEG-grafted chains
van der Waals attractive forces between the particles in close proximity	present	not present for the larger separation distance between the surfaces of the modified particles
friction force between the particles in the chains	significant: owing to strong attraction between the particles and their rough surface	small: because of lower attraction between the particles, smooth surface of and low friction between the PEG brushes
compensation of magnetic particle−particle interaction	absent	partially compensated by the repulsive steric forces between the PEG brushes
estimated distance between centers of the particles in the chains	∼100 nm	∼180 nm
estimated strength of magnetic interaction between the particles	−50 kT	−8 kT

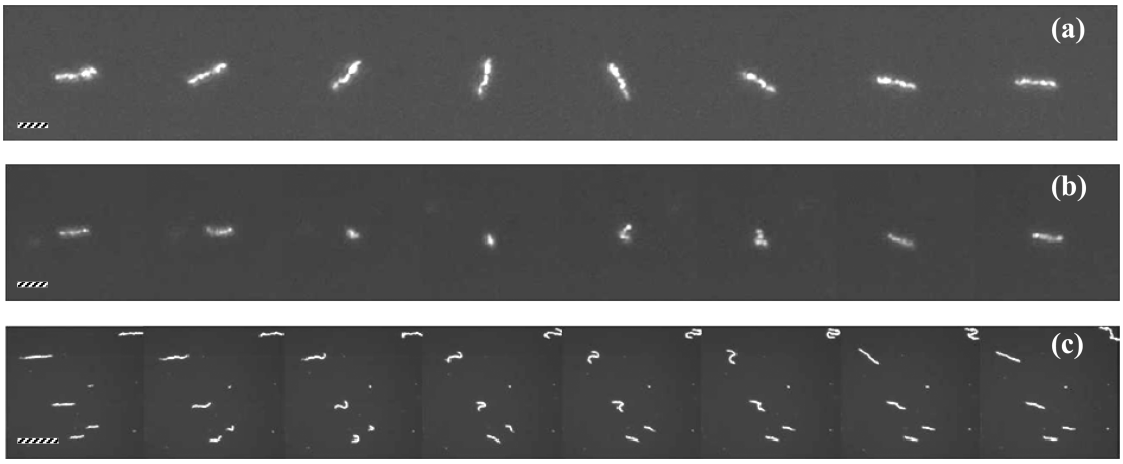

Figure 6. Dark-field microscopy images of the smaller chains formed by (a) as-synthesized (scale bar, 5 μm), (b) PEG-modified (scale bar, 5 μm) particles, and (c) larger multilayer chains formed by modified nanoparticles (scale bar, 50 μm). The direction of the magnetic field changes from left to right.

In this study, a relatively weak magnetic field of 10 G was used to support the chain formation. An even weaker (1−2 G) field was employed to manipulate the preformed chains. Original, unmodified Ni nanoparticles in the presence of an external magnetic field readily form chains and less-structured aggregates. Upon changing the direction of the field, such chains rotate (aligning the magnetic moment along the field). The motion does not involve any significant changes in geometrical dimensions or shape of the chains, revealing their rigidity (Figure 6a; see online Supporting Information for the video recording of the process). The particles constituting the chain are in direct contact with each other and form strong "stiffening" connections due to the powerful magnetic dipole−dipole interactions and direct surface contacts. In essence, the chain behaves as a single nickel nanorod.

On the contrary, a small chain composed of PEG-modified nanoparticles demonstrates quite remarkable behavior. Upon changing the direction of the field and inevitably going through a zero-field point, such chains undergo a chain−globule−chain transformation (Figure 6b; see online Supporting Information for the video recording of the process). Initially aligned along the field, the chain loses its rod-like structure and collapses (*via* self-folding) in the absence of a magnetic field. The "globular" structure is very dynamic, and the particles constituting the globe move vigorously. The transformation indicates the extreme flexibility of the chains.

An even more visually striking example of this unique chain flexibility was observed for multilayer larger chains formed of modified nanoparticles (Figure 6c; see online Supporting Information for the video recording of the process). The chains can bend to a high degree, attaining "snake-like" conformations. It is evident that the presence of a polymer layer on the nanoparticles' surface is a primary reason for such behavior.

CONCLUSIONS

We demonstrated that through synthesis of a specially designed grafted polymer layer on the surface of ferromagnetic nanoparticles it is possible to change fundamental behavior of the chains made of the nanoparticles. Namely, the fabricated flexible chains

possess the ability to adapt other than the typically observed rigid (nearly) straight configurations in the absence of an external magnetic field. The dynamic mobility of the ferromagnetic chains originates from the layer of the grafted PEG macromolecules enveloping each nanoparticle in the chain. While ferromagnetic chains of unmodified Ni nanoparticles behave as stiff nickel nanorods, the chains made of the grafted nanoparticles demonstrate extreme flexibility. Upon changing the direction of the field and inevitably going through a zero-field point, the shorter chains undergo a chain−globule−chain transformation. The longer chains can bend to a high degree, attaining "snake-like" configurations. To the best of our knowledge, it is the first time such extreme flexibility has been demonstrated for chains of ferromagnetic particles.

METHODS

Nickel Nanoparticles and Film. Nickel nanoparticles were synthesized *via* the reduction of nickel chloride with hydrazine at room temperature in an absolute alcohol environment, following the experimental procedure by Wu *et al.*[48] Reagent grade nickel chloride hexahydrate (Acros Organics), 80 wt % hydrazine monohydrate solution (Sigma-Aldrich), potassium hydroxide (Sigma-Aldrich), absolute ethanol (Acros Organics), and acetone (Sigma-Aldrich) were used in the synthesis. Specifically, 10 mL of 0.111 M solution of nickel chloride hexahydrate was prepared by dissolving an appropriate amount of the hexahydrate in absolute ethanol (mixture A). In a separate glass vial, a mixture of potassium hydroxide and hydrazine hydrate was prepared (mixture B). The amount of pure hydroxide (0.622 g) and pure hydrazine hydrate (0.278 g) was calculated in order to achieve a 1:5:10 $Ni^{2+}/N_2H_2/KOH$ molar ratio. The actual amounts of the reagents added were adjusted taking into consideration their purity stated by the suppliers. Mixture A was added to mixture B under vigorous magnetic stirring, and the vial was closed. The reagents were stirred at room temperature for 5 h. Obtained black precipitate (containing Ni nanoparticles) was cleaned of residues with DI water by repetitive centrifugation−redispersion process (at least four times). After the cleaning, the particles were transferred to acetone using the centrifugation−redispersion process.

For the model studies, silicon wafers covered with Ni film obtained by physical vapor deposition were employed. Prior to grafting, the wafer with the Ni film was cleaned using plasma cleaner (Harrick Scientific Corp.) and rinsed with DI water and ethanol.

Grafting. The nanoparticles and wafers were modified utilizing a grafting to technique that was previously employed in our laboratory for the surface modification of flat surfaces and nanoparticles.[64,70,71] PGMA (M_n = 176 kDa) and carboxyl-terminated PEG (M_n = 5000 kDa), made from PEG monomethyl ether (Sigma-Aldrich), were synthesized according to the published procedure.[64]

A layer of PGMA was deposited on the surface of the wafer by dip-coating from 1% acetone solution (dip coater, Mayer Fientechnik D-3400). The samples were annealed for 30 min at 60 °C. Then, the wafer was rinsed in acetone four times to remove unattached polymer. In the next step, the powder of the carboxyl-terminated PEG was deposited on the surface of a clean glass slide and covered with the wafer modified by the PGMA anchoring layer. The sample was annealed at 110 °C under vacuum for 2 h. Finally, the glass was removed (when PEG was still in melted state), and the wafer was rinsed four times in acetone to remove ungrafted polymer.

To modify Ni nanoparticles, the solution of PGMA in acetone (1 wt %, 10 mL) was prepared in 50 mL glass flask. The dispersion of Ni nanoparticles in acetone (10 mL, 0.25 wt %) was added dropwise to the PGMA solution under continuous sonication. The resulting mixture was sonicated for an additional 30 min. Then, the mixture was transferred to a 50 mL glass flask and rotary evaporated in a stream of nitrogen at room temperature until apparent removal of the solvent (about 1 h). The obtained PGMA−Ni nanoparticle composite film was vacuumed for 1 h in order to ensure complete removal of acetone. Next, the layer was annealed at 60 °C under vacuum for 30 min. After the annealing, the layer was subjected to acetone in order to dissolve a residual PGMA. The unreacted PGMA was additionally removed by repetitive centrifugation−redispersion process (at least four times) using acetone. After being cleaned, the modified particles were stored in acetone.

For the further modification of Ni nanoparticles, the solution of carboxy-terminated PEG in acetone (1 wt %, 7 mL) was prepared in a 20 mL glass vial. The dispersion of Ni nanoparticles in acetone (7 mL, 0.25 wt %) was added dropwise to the PEG solution under continuous sonication. The resulting mixture was sonicated for an additional 30 min. Then, it was transferred to a 50 mL glass flask and rotary evaporated in a stream of nitrogen at room temperature until apparent removal of the solvent (about 1 h). The obtained PGMA−Ni nanoparticle−PEG composite layer was vacuumed for 1 h in order to ensure complete removal of acetone. The layer was annealed at 110 °C under vacuum for 2 h. After the annealing, the layer was exposed to acetone in order to dissolve ungrafted PEG. The unreacted PEG was additionally removed by repetitive centrifugation−redispersion process (at least four times) using acetone. After being cleaned, the modified particles were stored in acetone.

Characterization. Synthesized and modified Ni particles were imaged using scanning electron microscopy (SEM S4800, Hitachi Inc.) and transmission electron microscopy (TEM H9500, Hitachi Inc.). Their crystal structure and magnetic properties were characterized by XRD (Ultima IV, Rigaku Corp.) and magnetometry (MicroMag, Cambridge Measurements Corp.). Ellipsometric measurements were conducted with a COMPEL automatic ellipsometer (InOmTech, Inc.) at a 70° angle of incidence. The refractive index used to calculate the thickness of PGMA was 1.525.[62] The refractive index for PEG was obtained from the supplier (n = 1.465). AFM imaging was conducted using a Dimension 3100 (Digital Instruments, Inc.) operated in the tapping mode.

The chain formation was observed using a homemade setup. Specifically, a 30 μm deep cell was made by etching a 25 × 25 mm microscope glass slide. A solution drop (~10 μL) was placed on a regular microscope glass slide and covered with the cell. The samples were observed using an Olympus BX51 microscope in a dark-field mode at 50× magnification. A Diagnostic Instruments, Inc. SPOT CCD camera was used for recording the images. The linear field of view was 150 μm. The magnetic field was generated using two coils with metal inserts spaced at about 2 cm and the sample holder in between.

Conflict of Interest: The authors declare no competing financial interest.

Acknowledgment. This work was supported by the Air Force Office of Scientific Research (Grant Numbers FA9550-12-1-0459 and FA8650-09-D-507 5900) and in part by the National Science Foundation (Grant Numbers DMR- 1107786 and CMMI-0825773). The authors thank Mr. Yu Gu and Prof. Konstantin G. Kornev from the Department of Materials Science and Engineering (Clemson University) for fruitful discussions and assistance with magnetic characterization.

Supporting Information Available: A video recording of the conformational changes of the chains formed by modified Ni nanoparticles. This material is available free of charge *via* the Internet at http://pubs.acs.org.

REFERENCES AND NOTES

1. Haw, M. D. Growth Kinetics of Colloidal Chains and Labyrinths. *Phys. Rev. E* **2010**, *81*, 031402/1–031402/7.
2. Klinkova, A.; Therien-Aubin, H.; Choueiri, R. M.; Rubinstein, M.; Kumacheva, E. Colloidal Analogs of Molecular Chain Stoppers. *Proc. Natl. Acad. Sci. U.S.A.* **2013**, *110*, 18775–18779.
3. Pyun, J. Nanocomposite Materials from Functional Polymers and Magnetic Colloids. *Polym. Rev.* **2007**, *47*, 231–263.
4. de Gennes, P. G.; Pincus, P. A. Pair Correlations in a Ferromagnetic Colloid. *Phys. Kondens. Mater.* **1970**, *11*, 189–198.
5. Choueiri, R. M.; Klinkova, A.; Therien-Aubin, H.; Rubinstein, M.; Kumacheva, E. Structural Transitions in Nanoparticle Assemblies Governed by Competing Nanoscale Forces. *J. Am. Chem. Soc.* **2013**, *135*, 10262–10265.
6. Motornov, M.; Malynych, S. Z.; Pippalla, D. S.; Zdyrko, B.; Royter, H.; Roiter, Y.; Kahabka, M.; Tokarev, A.; Tokarev, I.; Zhulina, E.; *et al.* Field-Directed Self-Assembly with Locking Nanoparticles. *Nano Lett.* **2012**, *12*, 3814–3820.
7. Pyun, J. Self-Assembly and Colloidal Polymerization of Polymer–Nanoparticle Hybrids into Mesoscopic Chains. *Angew. Chem., Int. Ed.* **2012**, *51*, 12408–12409.
8. Vutukuri, H. R.; Demirors, A. F.; Peng, B.; van Oostrum, P. D. J.; Imhof, A.; van Blaaderen, A. Colloidal Analogues of Charged and Uncharged Polymer Chains with Tunable Stiffness. *Angew. Chem., Int. Ed.* **2012**, *51*, 11249–11253.
9. Smallenburg, F.; Vutukuri, H. R.; Imhof, A.; van Blaaderen, A.; Dijkstra, M. Self-Assembly of Colloidal Particles into Strings in a Homogeneous External Electric or Magnetic Field. *J. Phys.: Condens. Matter* **2012**, *24*, 464113/1–464113/10.
10. Li, D.; Banon, S.; Biswal, S. L. Bending Dynamics of DNA-Linked Colloidal Particle Chains. *Soft Matter* **2010**, *6*, 4197–4204.
11. Tierno, P.; Sagues, F.; Johansen, T. H.; Sokolov, I. M. Evidence of Rouse-like Dynamics in Magnetically Ratchetting Colloidal Chains. *Soft Matter* **2011**, *7*, 7944–7947.
12. Butter, K.; Bomans, P. H. H.; Frederik, P. M.; Vroege, G. J.; Philipse, A. P. Direct Observation of Dipolar Chains in Iron Ferrofluids by Cryogenic Electron Microscopy. *Nat. Mater.* **2003**, *2*, 88–91.
13. Benkoski, J. J.; Bowles, S. E.; Korth, B. D.; Jones, R. L.; Douglas, J. F.; Karim, A.; Pyun, J. Field Induced Formation of Mesoscopic Polymer Chains from Functional Ferromagnetic Colloids. *J. Am. Chem. Soc.* **2007**, *129*, 6291–6297.
14. Eiji, K.; Tatsuya, O.; Takeru, K.; Suguru, S.; Makoto, M.; Hideto, Y.; Mikio, K.; Chiharu, M.; Shinji, H.; Keiichi, Y.; *et al.* Ferromagnetic Nanoparticles for Magnetic Hyperthermia and Thermoablation Therapy. *J. Phys. D: Appl. Phys.* **2010**, *43*, 474011/1–474011/9.
15. Guo, D.; Wu, C.; Li, X.; Jiang, H.; Wang, X.; Chen, B. *In Vitro* Cellular Uptake and Cytotoxic Effect of Functionalized Nickel Nanoparticles on Leukemia Cancer Cells. *J. Nanosci. Nanotechnol.* **2008**, *8*, 2301–2307.
16. Ibrahim, E. M. M.; Hampel, S.; Kamsanipally, R.; Thomas, J.; Erdmann, K.; Fuessel, S.; Taeschner, C.; Khavrus, V. O.; Gemming, T.; Leonhardt, A.; *et al.* Highly Biocompatible Superparamagnetic Ni Nanoparticles Dispersed in Submicron-Sized C Spheres. *Carbon* **2013**, *63*, 358–366.
17. Kumar, N. A.; Rejinold, N. S.; Anjali, P.; Balakrishnan, A.; Biswas, R.; Jayakumar, R. Preparation of Chitin Nanogels Containing Nickel Nanoparticles. *Carbohydr. Polym.* **2013**, *97*, 469–474.
18. Zhang, R.; Olin, H. In *Magnetic Nanoparticles in Biomedical Applications*; CRC Press: Boca Raton, FL, 2011; pp 119–139.
19. Rodriguez-Llamazares, S.; Merchan, J.; Olmedo, I.; Marambio, H. P.; Munoz, J. P.; Jara, P.; Sturm, J. C.; Chornik, B.; Pena, O.; Yutronic, N.; *et al.* Ni/Ni Oxides Nanoparticles with Potential Biomedical Applications Obtained by Displacement of a Nickel–Organometallic Complex. *J. Nanosci. Nanotechnol.* **2008**, *8*, 3820–3827.
20. Mironov, V. L.; Ermolaeva, O. L. Optimization of a Data Storage System Based on the Array of Ferromagnetic Particles and Magnetic Force Microscope. *J. Surf. Invest.: X-Ray, Synchrotron Neutron Tech.* **2009**, *3*, 840–845.
21. Abdel Hameed, R. M. Amperometric Glucose Sensor Based on Nickel Nanoparticles/Carbon Vulcan XC-72R. *Biosens. Bioelectron.* **2013**, *47*, 248–257.
22. Lin, K.-C.; Lin, Y.-C.; Chen, S.-M. A Highly Sensitive Non-enzymatic Glucose Sensor Based on Multi-walled Carbon Nanotubes Decorated with Nickel and Copper Nanoparticles. *Electrochim. Acta* **2013**, *96*, 164–172.
23. Liu, Y.; Zhang, L.; Guo, Q.; Hou, H.; You, T. Enzyme-Free Ethanol Sensor Based on Electrospun Nickel Nanoparticle-Loaded Carbon Fiber Paste Electrode. *Anal. Chim. Acta* **2010**, *663*, 153–157.
24. Malone, M. A.; Luthra, A.; Lioi, D.; Coe, J. V. Developing Plasmonics under the Infrared Microscope: From Ni Nanoparticle Arrays to Infrared Micromesh. *J. Phys. Chem. Lett.* **2012**, *3*, 1774–1782.
25. Weidong, Q.; Luyan, Z.; Gang, C. Magnetic Loading of Graphene–Nickel Nanoparticle Hybrid for Electrochemical Sensing of Carbohydrates. *Biosens. Bioelectron.* **2013**, *42*, 430–433.
26. Sreekumari, A.; Ilg, P. Slow Relaxation in Structure-Forming Ferrofluids. *Phys. Rev. E* **2013**, *88*, 042315/1–042315/9.
27. Santiago-Quinones, D. I.; Raj, K.; Rinaldi, C. A Comparison of the Magnetorheology of Two Ferrofluids with Different Magnetic Field-Dependent Chaining Behavior. *Rheol. Acta* **2013**, *52*, 719–726.
28. Mary, A. P. R.; Sandeep, C. S. S.; Narayanan, T. N.; Philip, R.; Moloney, P.; Ajayan, P. M.; Anantharaman, M. R. Nonlinear and Magneto-optical Transmission Studies on Magnetic Nanofluids of Non-interacting Metallic Nickel Nanoparticles. *Nanotechnology* **2011**, *22*, 375702/1–375702/7.
29. Bliznyuk, V.; Singamaneni, S.; Sahoo, S.; Polisetty, S.; Xi, H.; Ch, B. Self-Assembly of Magnetic Ni Nanoparticles into 1D Arrays with Antiferromagnetic Order. *Nanotechnology* **2009**, *20*, 105606/1–105606/8.
30. Cheng, G.; Romero, D.; Fraser, G. T.; Hight Walker, A. R. Magnetic-Field-Induced Assemblies of Cobalt Nanoparticles. *Langmuir* **2005**, *21*, 12055–12059.
31. Liu, C.-M.; Guo, L.; Wang, R.-M.; Deng, Y.; Xu, H.-B.; Yang, S. Magnetic Nanochains of Metal Formed by Assembly of Small Nanoparticles. *Chem. Commun.* **2004**, 2726–2727.
32. Tripp, S. L.; Pusztay, S. V.; Ribbe, A. E.; Wei, A. Self-Assembly of Cobalt Nanoparticle Rings. *J. Am. Chem. Soc.* **2002**, *124*, 7914–7915.
33. Nepijko, S. A.; Kutnyakhov, D.; Protsenko, I. E.; Elmers, H. J.; Schoenhense, G. Structure and Magnetic Properties of One-Dimensional Chains of Ferromagnetic Nanoparticles. *Appl. Phys. A: Mater. Sci. Process.* **2012**, *109*, 699–702.
34. Dreyfus, R.; Baudry, J.; Roper, M. L.; Fermigier, M.; Stone, H. A.; Bibette, J. Microscopic Artificial Swimmers. *Nature* **2005**, *437*, 862–865.
35. Cebers, A. Flexible Magnetic Filaments. *Curr. Opin. Colloid Interface Sci.* **2005**, *10*, 167–175.
36. Gauger, E.; Stark, H. Numerical Study of a Microscopic Artificial Swimmer. *Phys. Rev. E* **2006**, *74*, 021907/1–021907/10.
37. Roper, M.; Dreyfus, R.; Baudry, J.; Fermigier, M.; Bibette, J.; Stone, H. A. Do Magnetic Micro-swimmers Move Like Eukaryotic Cells? *Proc. R. Soc. A* **2008**, *464*, 877–904.
38. Biswal, S. L.; Gast, A. P. Mechanics of Semiflexible Chains Formed by Poly(ethylene glycol)-Linked Paramagnetic Particles. *Phys. Rev. E* **2003**, *68*, 021402/1–021402/9.
39. Biswal, S. L.; Gast, A. P. Micromixing with Linked Chains of Paramagnetic Particles. *Anal. Chem.* **2004**, *76*, 6448–6455.
40. Biswal, S. L.; Gast, A. P. Rotational Dynamics of Semiflexible Paramagnetic Particle Chains. *Phys. Rev. E* **2004**, *69*, 041406/1–041406/9.
41. Breidenich, J. L.; Wei, M. C.; Clatterbaugh, G. V.; Benkoski, J. J.; Keng, P. Y.; Pyun, J. Controlling Length and Areal Density of Artificial Cilia through the Dipolar Assembly of Ferromagnetic Nanoparticles. *Soft Matter* **2012**, *8*, 5334–5341.
42. Benkoski, J. J.; Bowles, S. E.; Jones, R. L.; Douglas, J. F.; Pyun, J.; Karim, A. Self-Assembly of Polymer-Coated Ferromagnetic Nanoparticles into Mesoscopic Polymer Chains. *J. Polym. Sci., Part B: Polym. Phys.* **2008**, *46*, 2267–2277.

43. Benkoski, J. J.; Breidenich, J. L.; Uy, O. M.; Hayes, A. T.; Deacon, R. M.; Land, H. B.; Spicer, J. M.; Keng, P. Y.; Pyun, J. Dipolar Organization and Magnetic Actuation of Flagella-like Nanoparticle Assemblies. *J. Mater. Chem.* **2011**, *21*, 7314–7325.
44. Benkoski, J. J.; Deacon, R. M.; Land, H. B.; Baird, L. M.; Breidenich, J. L.; Srinivasan, R.; Clatterbaugh, G. V.; Keng, P. Y.; Pyun, J. Dipolar Assembly of Ferromagnetic Nanoparticles into Magnetically Driven Artificial Cilia. *Soft Matter* **2010**, *6*, 602–609.
45. Goubault, C.; Jop, P.; Fermigier, M.; Baudry, J.; Bertrand, E.; Bibette, J. Flexible Magnetic Filaments as Micromechanical Sensors. *Phys. Rev. Lett.* **2003**, *91*, 260802/1–260802/4.
46. Cerda, J. J.; Sintes, T.; Toral, R. Pair Interaction between End-Grafted Polymers onto Spherical Surfaces: A Monte Carlo Study. *Macromolecules* **2003**, *36*, 1407–1413.
47. Tsyalkovsky, V.; Burtovyy, R.; Klep, V.; Lupitskyy, R.; Motornov, M.; Minko, S.; Luzinov, I. Fluorescent Nanoparticles Stabilized by Poly(ethylene glycol) Containing Shell for pH-Triggered Tunable Aggregation in Aqueous Environment. *Langmuir* **2010**, *26*, 10684–10692.
48. Wu, Z. G.; Munoz, M.; Montero, O. The Synthesis of Nickel Nanoparticles by Hydrazine Reduction. *Adv. Powder Technol.* **2010**, *21*, 165–168.
49. Jette, E. R.; Foote, F. Precision Determination of Lattice Constants. *J. Chem. Phys.* **1935**, *3*, 605–616.
50. Lifshin, E. *X-ray Characterization of Materials*, 1 ed.; Wiley-VCH: Weinheim, Germany, 1999.
51. O'Handley, R. C. *Modern Magnetic Materials: Principles and Applications*; Wiley: New York, 2000.
52. Lu, H. M.; Zheng, W. T.; Jiang, Q. Saturation Magnetization of Ferromagnetic and Ferrimagnetic Nanocrystals at Room Temperature. *J. Phys. D: Appl. Phys.* **2007**, *40*, 320–325.
53. Israelachvili, J. N. *Intermolecular and Surface Forces*, 2nd ed.; Academic Press: London, 1991.
54. Nommensen, P. A.; Duits, M. H. G.; van den Ende, D.; Mellema, J. Steady Shear Behavior of Polymerically Stabilized Suspensions: Experiments and Lubrication Based Modeling. *Phys. Rev. E* **1999**, *59*, 3147–3154.
55. Phan, S. E.; Russel, W. B.; Cheng, Z. D.; Zhu, J. X.; Chaikin, P. M.; Dunsmuir, J. H.; Ottewill, R. H. Phase Transition, Equation of State, and Limiting Shear Viscosities of Hard Sphere Dispersions. *Phys. Rev. E* **1996**, *54*, 6633–6645.
56. Napper, D. H. *Polymeric Stabilization of Colloidal Dispersions*; Academic Press: London, 1983.
57. Kuhl, T. L.; Leckband, D. E.; Lasic, D. D.; Israelachvili, J. N. Modulation of Interaction Forces between Bilayers Exposing Short-Chained Ethylene-Oxide Headgroups. *Biophys. J.* **1994**, *66*, 1479–1488.
58. Lai, P. Y.; Binder, K. Structure and Dynamics of Grafted Polymer Layers: A Monte-Carlo Simulation. *J. Chem. Phys.* **1991**, *95*, 9288–9299.
59. Murat, M.; Grest, G. S. Interaction between Grafted Polymeric Brushes: A Molecular-Dynamics Study. *Phys. Rev. Lett.* **1989**, *63*, 1074–1077.
60. Dupas, C.; Houdy, P.; Lahmani, M. *Nanoscience: Nanotechnologies and Nanophysics*; Springer-Verlag: Berlin, 2007; p 505.
61. Qi, L.; Fresnais, J.; Muller, P.; Theodoly, O.; Berret, J. F.; Chapel, J. P. Interfacial Activity of Phosphonated-PEG Functionalized Cerium Oxide Nanoparticles. *Langmuir* **2012**, *28*, 11448–11456.
62. Zdyrko, B.; Varshney, S. K.; Luzinov, I. Effect of Molecular Weight on Synthesis and Surface Morphology of High-Density Poly(ethylene glycol) Grafted Layers. *Langmuir* **2004**, *20*, 6727–6735.
63. Zdyrko, B.; Klep, V.; Luzinov, I. Synthesis and Surface Morphology of High-Density Poly(ethylene glycol) Grafted Layers. *Langmuir* **2003**, *19*, 10179–10187.
64. Tsyalkovsky, V.; Klep, V.; Ramaratnam, K.; Lupitskyy, R.; Minko, S.; Luzinov, I. Fluorescent Reactive Core−Shell Composite Nanoparticles with a High Surface Concentration of Epoxy Functionalities. *Chem. Mater.* **2008**, *20*, 317–325.
65. Hoy, O.; Zdyrko, B.; Lupitskyy, R.; Sheparovych, R.; Aulich, D.; Wang, J. F.; Bittrich, E.; Eichhorn, K. J.; Uhlmann, P.; Hinrichs, K.; *et al.* Synthetic Hydrophilic Materials with Tunable Strength and a Range of Hydrophobic Interactions. *Adv. Funct. Mater.* **2010**, *20*, 2240–2247.
66. Blank, W. J.; He, Z. A.; Picci, M. Catalysis of the Epoxy-Carboxyl Reaction. *J. Coat. Technol.* **2002**, *74*, 33–41.
67. Drobek, T.; Spencer, N. D. Nanotribology of Surface-Grafted PEG Layers in an Aqueous Environment. *Langmuir* **2007**, *24*, 1484–1488.
68. Yan, X.; Perry, S. S.; Spencer, N. D.; Pasche, S. p.; De Paul, S. M.; Textor, M.; Lim, M. S. Reduction of Friction at Oxide Interfaces upon Polymer Adsorption from Aqueous Solutions. *Langmuir* **2003**, *20*, 423–428.
69. Butter, K.; Bomans, P. H.; Frederik, P. M.; Vroege, G. J.; Philipse, A. P. Direct Observation of Dipolar Chains in Ferrofluids in Zero Field Using Cryogenic Electron Microscopy. *J. Phys.: Condens. Matter* **2003**, *15*, S1451–S1470.
70. Zdyrko, B.; Luzinov, I. Polymer Brushes by the "Grafting to" Method. *Macromol. Rapid Commun.* **2011**, *32*, 859–869.
71. Iyer, K. S.; Luzinov, I. Effect of Macromolecular Anchoring Layer Thickness and Molecular Weight on Polymer Grafting. *Macromolecules* **2004**, *37*, 9538–9545.